Resonate and fire dynamics in Complex Oscillation Based Test of analog filters

This is the author's version of the article that has been presented at IEEE ISCAS2011
The editorial version of the paper is available at http://dx.doi.org/10.1109/ISCAS.2011.5937817

Resonate and Fire Dynamics in Complex Oscillation Based Test of Analog Filters

Sergio Callegari
ARCES and DEIS
University of Bologna
scallegari@arces.unibo.it

Fabio Pareschi
ENDIF
University of Ferrara;
fabio.pareschi@unife.it

Gianluca Setti
ENDIF
University of Ferrara; and
ARCES
University of Bologna
gianluca.setti@unife.it

Mani Soma
EE
University of Washington
manisoma@u.washington.edu

***Abstract*—Recently, proposals have been made for enhancing the Oscillation Based Test (OBT) methodology by using non-plain oscillation regimes, leading to so called Complex Oscillation Based Test (COBT). Here we focus on a recently illustrated strategy for the testing of analog 2nd order filters, showing that the COBT dynamics is quite similar to that expressed by Resonate & Fire (R+F) neuron models. In this interpretation, the testing approach can be related to firing-rate measures. A brief description is given of the mathematical models necessary to achieve a precise characterization of firing times, showing how it can be used for testing purposes. A practical example with simulation data is also provided.**

I. Introduction

Oscillation Based Test (OBT) is a technique introduced in the late '90s to address the increasing costs associated with the testing of analog subsystems in large mixed-mode ICs and Systems on a Chip (SOCs) [1]. Savings are made by avoiding the need of dedicated circuits or signal injection point for exciting the Blocks Under Test (BUTs). This is achieved by turning the BUTs themselves into oscillators whose features can reveal faults [2]. Costs can be further reduced by characterizing the oscillations only by means of quantities that are inherently expressed in the time domain, so that data acquisition can be directly practiced by counters and no A/D converters are required for testing.

In typical deployments, OBT oscillation regimes are plain sinusoidal. Consequently, the only time-domain quantity at hand is the oscillation period. Relying on this single measurand is known to limit the achievable fault coverage [2], [3] and to hinder most forms of functional testing [4, and references therein]. To overcome these issues, the usage of non-plain oscillation regimes (including long-period-non-sinusoidal, multi-periodic or chaotic) has recently been proposed under the name of Complex Oscillation Based Test (COBT) [5], [6].

Given that COBT can be considered a super-set of OBT, the spectrum of COBT techniques can obviously be quite large. So far, ideas have been presented for data-converters [5] and analog filters [6]. In [4], an attempt has been made at defining a general strategy for achieving multiple time-domain measurands via COBT from analog BUTs. The strategy is particularly suited at blocks where the initial behavior is already based on resonance phenomena (as in many types of filters).

Here, we re-interpret this latest approach, by noticing that the dynamical features being exploited are actually quite similar to those found in so called Resonate & Fire (R+F) neuron models [7] and Chaotic Spiking Oscillators (CSOs) [8], [9]. Intriguingly, in this interpretation the time-domain measurands being gathered for testing purposes correspond to the firing rates. The inherent scenario sees the "neuron" fed by stationary inputs, while parameter changes in the BUT get converted into model variations, that induce changes in the average firing rates.

In this paper, by studying the R+F (or CSO) dynamics by the statistical approach in [10], we can accurately characterize the BUT parameters to firing-rate relationships. Once inverted, such relationships offer a means to functionally/parametrically check the BUT against its nominal specifications. The current analysis represents a significant step ahead of previously presented models [4] that were based on relatively rough approximations. To aid comparison, simulation data is provided with regards to the same sample circuits.

II. Background

A. COBT of a bandpass filter

Fig. 1 illustrates the Band-pass (BP) filter used as a benchmark for the present discussion. It is the same 2nd order switched

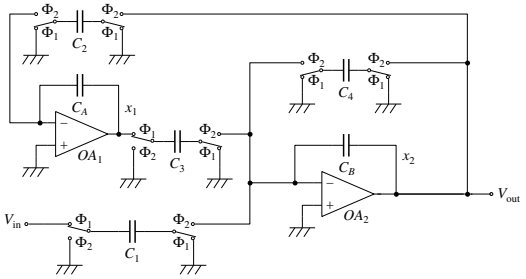

Figure 1: The filter used as an example.

capacitor circuit adopted in [4]. When clocked at a sufficiently high rate $f_\Phi \gg f_0$ (where f_0 is the center band frequency) it can accurately emulate a Continuous-Time (CT) transfer function such as:

$$H(s) = G_0 \frac{\frac{2\pi f_0}{Q} s}{s^2 + \frac{2\pi f_0}{Q} s + (2\pi f_0)^2} \tag{1}$$

where Q is the merit factor, G_0 is the center band gain, and

$$\frac{f_0}{f_\Phi} = \frac{1}{2\pi}\sqrt{\frac{C_2 C_3}{C_A C_B}} \quad G_0 = \frac{C_1}{C_4} \quad Q = \frac{1}{C_4}\sqrt{\frac{C_2 C_3 C_B}{C_A}} \tag{2}$$

This is the author's version of the article that has been presented at IEEE ISCAS2011
The editorial version of the paper is available at http://dx.doi.org/10.1109/ISCAS.2011.5937817

In the following, for the sake of brevity, the discussion will directly rely on the CT model.[1]

Fig. 2 shows the same filter as in Fig. 1 once modified for COBT as in [4]. The effect of the changes are the following.

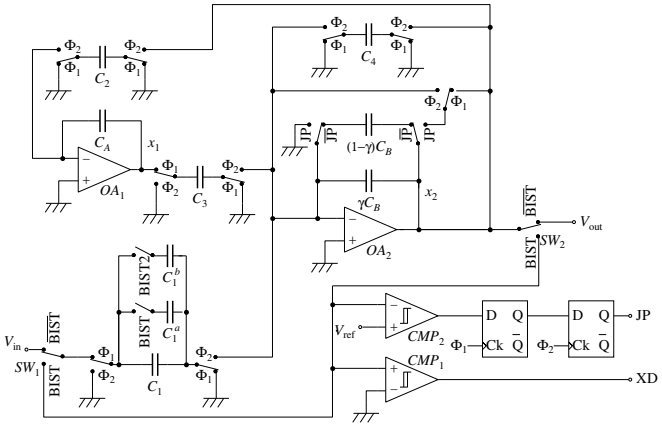

Figure 2: The filter modified for COBT.

First, the two switches SW_1, SW_2 allow the filter to become part of a loop when in test mode (BIST signal asserted). Secondly, capacitors C_1, C_{1a} and C_{1b} allow to control the loop gain among two different values $G_{L\,a|b} = (C_1+C_{1\,a|b})/C_4$, both larger than 1 and capable to assure that the system will diverge from the equilibrium point created by the above loop. Specifically, one has

$$G_{L\,a|b} = G_0 \cdot \left(1 + \frac{C_{1\,a|b}}{C_1}\right) \tag{3}$$

where the ratio $C_{1\,a|b}/C_1$ can be set with good precision. Thirdly, comparator CMP_1 allows the zero crossings of the state variable x_2 (corresponding to the output of OA_2 and to V_{out}) to be observed from the digital signal XD. Finally, comparator CMP_2 allows tracking events when x_2 exceeds a given threshold V_{ref} by means of the digital signal JP (the two D-latches merely adjust the synchronization of JP to the clock). When JP is asserted, thanks to the split of capacitor C_B into γC_B and $(1-\gamma)C_B$ and to a couple of JP-driven switches in the local loop around OA_2, x_2 gets reset to a known value $V_{\text{reset}} \approx V_{\text{ref}}(2\gamma-1)/\gamma$, while the other state variable x_1, output of OA_1 is unaffected. For further details see [4].

As a consequence of these changes, when the filter enters test mode, trajectories such as those in Fig. 3 are obtained. In practice, as long as x_2 does not exceed V_{ref}, one has a quasi-harmonic oscillatory behavior with increasing envelope. As soon as x_2 reaches V_{ref}, there is a sudden "jump" in the trajectory due to the reset of x_2. The state is almost instantaneously taken close to the system equilibrium point, so that the quasi-harmonic divergence can start again.

Altogether, one has an *autonomous impulsive differential system* [11] such as

$$\begin{cases} \boldsymbol{x}' = \boldsymbol{A}\boldsymbol{x} & x_2 > V_{\text{ref}} \\ \Delta\boldsymbol{x} = (0, V_{\text{reset}} - V_{\text{ref}})^{\mathrm{T}} & \text{otherwise} \end{cases} \tag{4}$$

[1]In principle, this is appropriate since the functional validation is typically to be performed against Eq. (1) anyway. However, it introduces some minor and easy to compensate systematic errors (as illustrated at the end of the paper), that shall be fully addressed in a future publication.

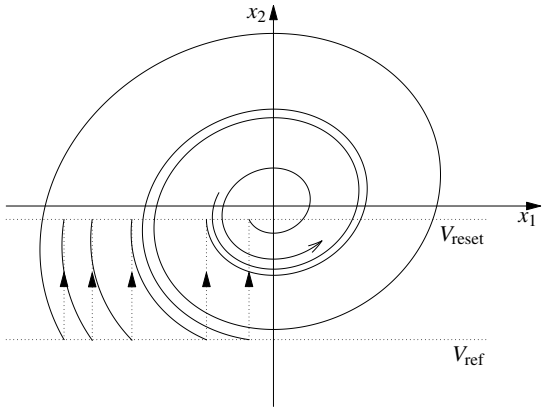

Figure 3: Sample COBT trajectories.

where $\boldsymbol{x} = (x_1, x_2)^{\mathrm{T}}$, $a_{1,1} = 0$, $a_{1,2} \approx -C_2 f_\Phi/C_A$, $a_{2,1} \approx C_3 f_\Phi/C_B$, $a_{2,2} \approx (-C_4+C_1+C_{1\,a|b}) f_\Phi/C_B$. Under this model, the state variables evolve as piece-wise exponentially-increasing sine-waves. Namely, as long as jumps are not exercised,

$$x_i(t) = A_i e^{\alpha t} \sin(\omega_0 t + \phi_i) \tag{5}$$

where $i \in \{1, 2\}$, A_i, ϕ_i are appropriate parameters related to initial conditions, ϕ_1 is in quadrature with ϕ_2, and $\omega_0 = 2\pi f_0$. Note that as long as this situation is exercised, XD can directly reveal f_0. Furthermore, the quantity α is given by the real part of the eigenvalues of $\boldsymbol{A}$ as:

$$\alpha = \frac{C_1 + C_{1\,a|b} - C_4}{2C_B} f_\Phi = \frac{\omega_0}{2Q}(G_{L\,a|b} - 1) \tag{6}$$

B. Resonate and fire (chaotic spiking) dynamics

It is now possible to make a parallel between the dynamics in Fig. 3 and that portrayed in [7] for R+F systems. The waveforms are remarkably similar since R+F systems also involve signals made of portion of exponential growing sinusoids (in the resonant phases) separated by sharp discontinuities (the firing events).

The parallel is interesting since in R+F neurons the firing activity is the major means by which information is encoded. The firing patterns fully incorporate both the effects of the input excitation and of the internal processing parameters. In absence of external inputs, as it is now the case, one can expect the firing to reveal many aspects of the internal neuron tuning and this is one of the reason why the observation of the "state jumps" seems a promising approach to validate the BUT operation in COBT.

In most conditions, R+F systems show firing events arranged in highly irregular patterns, where order can only be found by statistical means. Simplified, artificial models explain this as a manifestation of chaotic dynamics. Approaching R+F systems as CSOs [9], using a statistical toolbox [10], can thus be effective in tying averaged indicators to system parameters. In a COBT perspective, this is indispensable since COBT precisely aims at identifying system parameters from such indicators.

Due to the complexity of the nonlinear models inherent in CSOs, a common first step in the analysis is a model order reduction practiced by taking Poincare sections [8], [12]. The very existence of a thresholding mechanism in the model suggest a practical way to do so by building a *return map*, namely a function

This is the author's version of the article that has been presented at IEEE ISCAS2011
The editorial version of the paper is available at http://dx.doi.org/10.1109/ISCAS.2011.5937817

$M : \mathbb{R} \to \mathbb{R}$ tying to each other the subsequent intersections of the trajectories with the threshold.

III. Analysis of the firing rate

For the specific model in Eq. (4), the return map is a function M such that if $x(n)$ is the value that x_1 takes at the n-th firing event, then $x(n+1) = M(x(n))$ is the value of x_1 at the $(n+1)$-th firing. Unfortunately, it is impossible to express M in closed form using conventional mathematical operators. However, this can be done by devising ad hoc operators from an "exponential envelope" trigonometry. The actual way to do so is simple but cumbersome and will be discussed elsewhere. Here, it is sufficient to remark that the shape of M only depends on two adimensional parameters, namely the α/ω ratio and the $V_{\text{reset}}/V_{\text{ref}}$ ratio. As an example, Fig. 4 (top) show a sample return map. As long as

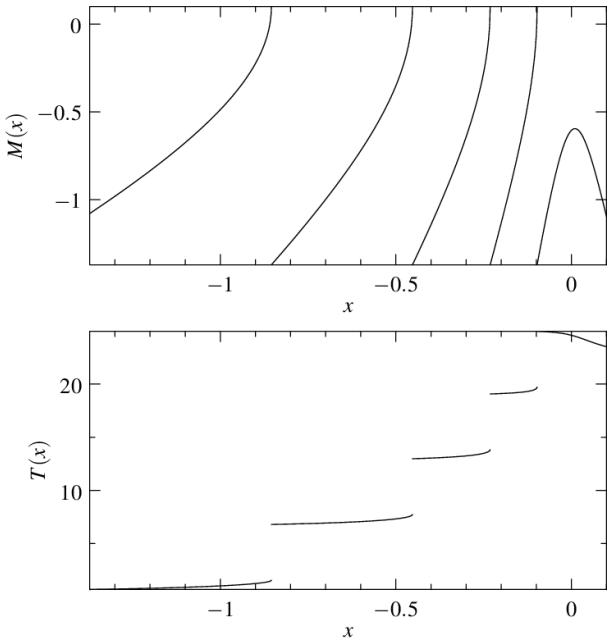

Figure 4: Return map (top) and firing time map (bottom) for $\alpha/\omega = 1/10$ and $V_{\text{reset}}/V_{\text{ref}} = 1/10$. The quantities V_{ref} and ω that merely act as scaling factors are normalized to one.

α/ω is sufficiently low (lower than approximately 0.18 in typical setups), the map admits an invariant set $\mathcal{I}$.

While the typical analysis of CSOs focuses on studying the return map properties capable to assure chaoticity (and possibly some bifurcation features) [8], here the goal is to express the dependency of the average firing rate on the system parameters. To this aim: (i) the conventional analysis of CSOs is here enhanced by the application of statistical analysis toolboxes such as those in [10]; and (ii) the return-map is coupled to a *firing-time-map* $T : \mathbb{R} \to \mathbb{R}$, such that if $x(n)$ is the value that x_1 takes at the n-th firing event, $t(n) = T(x(n))$ is the time taken to get to the next firing event. Fig. 4 (bottom) shows a sample firing-time-map.

Specifically, with regards to the first point, an approximated $N \times N$ *kneading matrix* [10] $\boldsymbol{K}$ is built, by partitioning $\mathcal{I}$ into N intervals I_i, with $i = 1 \dots N$. Entry $k_{i,j}$ of $\boldsymbol{K}$ is taken to indicate the fraction of I_i that maps into I_j. By construction, $\boldsymbol{K}$ is thus a *stochastic matrix* and as such it has a unitary eigenvalue. From [10, and references therein] it is known that if such eigenvalue has unitary multiplicity, then the corresponding eigenvector $\boldsymbol{P}$ (once its elements are normalized with regards to the lengths of the partition intervals so that their sum is 1), happens to (approximately) encode the probabilities by which x distributes over the many I_i when the iteration $x(n+1) = M(x(n))$ is started at non-pathological initial conditions. The approximation accuracy increases as the partitioning is refined.

For our experiments we have considered uniform partitions with N values up to 4096. Notably, from the observation of $\boldsymbol{K}$ one cannot generally *prove* whether M is chaotic or not (due to the approximated nature of the partitioning, though there are particular cases where "perfect" partitionings can be taken). Nonetheless, from the way in which the spectrum of $\boldsymbol{K}$ varies as N is increased, strong arguments "suggesting" chaoticity can be extrapolated. Specifically, as long as: (i) the multiplicity of the largest eigenvalue remains unitary; (ii) the gap between the second largest eigenvalue an the unitary circle does not close as N is increased; and (iii) $\boldsymbol{P}$ is not sparse, one can reasonably assume that the system is chaotic. In our system, this is the case, but for quite specific set of parameters, typically involving negative $V_{\text{reset}}/V_{\text{ref}}$ values.

By computing $\boldsymbol{K}$ and $\boldsymbol{P}$, one can thus find out how the starting points of the state jumps distribute when the COBT approach is practiced on the filter. A Probability Density Function (PDF) is derived as:

$$\rho(x) = p_i/\mu(\mathcal{I}) \text{ if } x \in I_i \tag{7}$$

where $\mu(\mathcal{I})$ is the length of $\mathcal{I}$. Figure 5 shows the PDF relative to the same conditions as in Fig. 4. Eventually, once $\rho(x)$ is known,

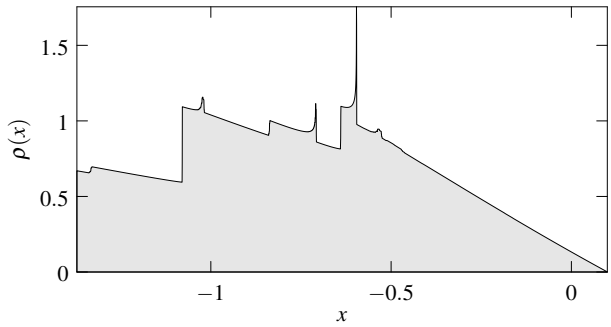

Figure 5: PDF for the same conditions as in Fig. 4. Plot obtained with a partition refinement index $N = 4096$.

the average period between successive firings can be found thanks to the firing-time-map T as

$$\overline{\tau} = \int_{\mathcal{I}} T(x)\rho(x)\,dx \tag{8}$$

What is most interesting is to relate $\overline{\tau}$ to α/ω as illustrated in Fig. 6. As it can be seen the relationship is almost hyperbolic (note that the abscissa is inverted in the graph for better representation), but not quite. From the plot it is evident that: (i) the experimental data is extremely well matched by the current model; (ii) the match is much more accurate that the previously proposed one [4], that was relying on a purely hyperbolic approximation and as such limited to a rather restricted interval of α values. Another interesting feature of the current model with regards to [4] is that

This is the author's version of the article that has been presented at IEEE ISCAS2011
The editorial version of the paper is available at http://dx.doi.org/10.1109/ISCAS.2011.5937817

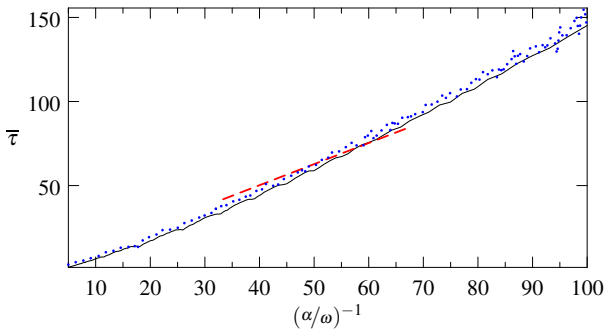

Figure 6: Dependency of $\overline{\tau}$ on α/ω, for $V_{\text{reset}}/V_{\text{ref}} = 1/10$. The quantity $(\alpha/\omega)^{-1}$ is reported on the abscissa to better visualize that the dependency is almost an inverse proportionality. Data obtained with the current analysis (solid line) is compared that that delivered by the approximated analysis in [4] (dashed line) and to data extrapolated from time-domain simulations with $f_\Phi/f_0 = 1000$ (dotted line).

it does not need to be tuned over experimental data (typically obtained by behavioral simulations). Consequently curves such as the solid line in Fig. 6 can be computed in an very efficient way. For instance, a few minutes of computation are enough on a current PC exploiting sparse matrix codes for the eigensystem solution (in comparison to several hours for models that need tuned over experimental data).

Once a relationship such as that in Fig. 6 is available, its exploitation for testing is rather straightforward. As already discussed in [4], one can collect two average firing rate periods $\overline{\tau}_{a|b}$ exploiting the two different loop capacitors $C_{1\,a|b}$ in the schematic of Fig. 2. From the two $\overline{\tau}_{a|b}$ two different $\alpha_{a|b}$ values can be estimated by inverting the relationship. Finally, by solving a system where equation (6) is used twice, together with (3), the values G_0 and Q can finally be obtained.

Table I shows some simulations data by which the above claim can be validated. Data is obtained from a filter that should be nominally tuned at $f_0 = 1\,\text{kHz}$, $G_0 = 1$, $Q = 5$, where mismatches and other non-idealities are on purpose applied to affect the operation. The table reports G_0 and Q values obtained by the present methodology and compares them to those obtained by a frequency sweep.

Table I: Experimental validation data from simulation.

Standard measure		Current estimation (I)		Current estimation (II)	
G_0	Q	G_0	Q	G_0	Q
0.99	4.50	1.01	5.54	1.01	4.6
1.08	4.62	1.11	5.92	1.11	4.9
0.92	5.16	0.93	5.72	0.93	4.8
1.03	4.63	1.04	5.60	1.04	4.6
0.98	5.92	0.99	7.07	0.99	5.9

As it can be seen from column (I), the estimation of G_0 is always almost perfect, while the estimation of Q is affected by a significant bias. Once this systematic error is removed as in column (II), also the estimation of Q becomes rather accurate. The bias is a consequence of the adoption of a CT modeling for a system that is in fact Discrete-Time (DT). In addition to typical CT/DT discrepancies, in the COBT setup there are also other. For instance state "jumps" or "firings" are compelled to happen with a clock-period delay. This effect is also visible from Fig. 6, where the solid curve (model) and the dotted data (experimental data) have a little slope difference. In any case, bias does not affect the usability of the proposed approach since, as illustrated, it can be easily empirically corrected. In a further publication, DT effects will be dealt with from start. An analysis of error propagation through the system of equations used to estimate G_0 and Q from $\alpha_{a|b}$ suggests that once biases are removed in the test conditions used from the table a 5 % uncertainty in the estimation of the average firing times can translate in approximately a 1 % uncertainty on G_0 and a 10 % uncertainty on Q.

IV. Conclusions

It has been shown that by taking advantage of tools from statistical nonlinear dynamics, the accuracy of a previously proposed methodology for the COBT of analog filters can be significantly improved. Furthermore, the dynamical system used for testing can be related to R+F and CSO models. The present analysis also allowed to identify some second order effects that appear when the circuit to be tested is DT. These will be more thoroughly analyzed in another forthcoming paper.

V. Acknowledgments

The research work was partially supported under the MIUR internationalization program "Applicazione della Dinamica Nonlineare alle Tecnologie dell'Informazione".

References

[1] K. Arabi and B. Kaminska, "Oscillation-test strategy for analog and mixed-signal integrated circuits," in *Proceedings of the 14th IEEE VLSI Test Symposium*, Princeton, NJ, May 1996, pp. 476–482.

[2] G. Huertas Sánchez, D. Vásquez García de la Vega, A. Rueda Rueda, and J. L. Huertas Díaz, *Oscillation-Based Test in Mixed-Signal Circuits*, ser. Frontiers in Electronic Testing. Dordrecht: Springer, 2006.

[3] M. W.-T. W. Wong, "On the issues of oscillation test methodology," *IEEE Trans. Instrum. Meas.*, vol. 49, no. 2, pp. 240–245, Apr. 2000.

[4] S. Callegari, F. Pareschi, G. Setti, and M. Soma, "Complex oscillation based test and its application to analog filters," *IEEE Trans. Circuits Syst. I*, vol. 57, no. 5, May 2010.

[5] S. Callegari, "Introducing *Complex Oscillation Based Test*: an application example targeting analog to digital converters," in *Proc. of ISCAS*, Seattle, WA (USA), May 2008, pp. 320–323.

[6] S. Callegari, G. Setti, and M. Soma, "Complex oscillation based test of analog filters," in *Proc. of ISCAS'09*, Taipei, TW, May 2009, pp. 2854–2857.

[7] E. M. Izhikevich, "Resonate-and-fire neurons," *Neural Networks*, vol. 14, no. 6-7 (special issue on Spiking Neurons in Neuroscience and Technology), pp. 883–894, Jul. 2001.

[8] K. Mitsubori and T. Saito, "Dependent switched capacitor chaos generator and its synchronization," *IEEE Trans. Circuits Syst. I*, vol. 44, no. 12, pp. 1122–1128, Dec. 1997.

[9] T. Inagaki and T. Saito, "Consistency in a chaotic spiking oscillator," *IEICE Trans. on Fundamentals*, vol. E91-A, no. 8, pp. 2040–2043, Aug. 2008.

[10] G. Setti, G. Mazzini, R. Rovatti, and S. Callegari, "Statistical modeling of discrete time chaotic processes: Basic finite dimensional tools and applications," *Proc. IEEE*, vol. 90, no. 5, pp. 662–690, May 2002.

[11] V. Lakshmikantham, *Theory of Impulsive Differential Equations*, ser. Modern Applied Mathematics. World Scientific, 1989.

[12] E. Ott, *Chaos in dynamical systems*. Cambridge University Press, 1993.